ChemPubSoc Europe

DOI: 10.1002/ejic.201600223

EurJIC European Journal of Inorganic Chemistry

Full Paper

Rare-Earth Chemistry

Scandium Complexes Bearing Bis(oxazolinylphenyl)amide Ligands: An Analysis of Their Reactivity, Solution-State Structures and Photophysical Properties

Stacey D. Bennett,[a] Simon J. A. Pope,[a] Robert L. Jenkins,[a] and Benjamin D. Ward*[a]

Abstract: The coordination chemistry of scandium supported by bis(oxazolinylphenyl)amide (R-BOPA) ligands is reported. The R-BOPA ligand is too sterically demanding to afford bis(amide) complexes [Sc(R-BOPA){$N(SiMe_3)_2$}$_2$], but reaction of the protio-ligand with [Sc{$N(SiMe_3)_2$}$_2$Cl(THF)] (**1**) afforded the mixed amido-chloride complexes [Sc(R-BOPA){$N(SiMe_3)_2$}Cl] (**2**). The selective reaction of the amido and chloride co-ligands in **2** has been investigated; whilst the chloride ligand can be removed cleanly by metathesis, protonation of the $N(SiMe_3)_2$ ligand results in competitive protonation of the R-BOPA ligand. The complexes [Sc(R-BOPA)(CH_2SiMe_2Ph)$_2$] (**5**) have been synthesised. Each R-BOPA-containing complex exists in two isomeric forms. The equilibrium has been investigated both experimentally and computationally, and the data suggest that a concerted rotation of the phenyl rings interconverts the two diastereomeric isomers. All of the R-BOPA complexes were found to be luminescent; an analysis of the photophysics, aided by TD-DFT calculations, suggests ligand-centred luminescence with distinct emission lifetimes for each isomer.

Introduction

Organometallic-type complexes of the rare-earth metals (including Group 3 and lanthanide elements) have been the focus of intense study for their functional behaviour, particularly in homogeneous catalysis.[1–13] To expedite the development of functional rare-earth complexes, we must first thoroughly probe their organometallic and coordination chemistry (including stoichiometric reaction chemistry) with a range of supporting ligand environments. Such studies provide invaluable information relating to coordination geometries, ligand stability, and viable reaction pathways; all of which are crucial in understanding complex molecular processes. Whilst the coordination chemistry of the rare-earth metals is generally well-understood, there are still ligand classes that are under-represented, as a fraction of the total knowledge-base; oxazoline-containing ligands are a pertinent example.[11]

Scandium complexes often show greater thermal stability than analogous complexes containing other rare-earth ions.[14–16] Therefore the study of scandium can be used to discern the key parameters relating to a particular ligand type, and often precedes developments with the other, more challenging, lanthanide metals. This feature of scandium chemistry is often attributed to the relatively small ionic radius of scandium (0.75 Å) compared to the other metals in the series (0.86–1.03 Å).[11,17] Specific recent examples of scandium complexes being employed in this manner include the first report of a terminal scandium terminal imido complex;[18] the knowledge thus acquired was instrumental in extending this chemistry to yttrium and lutetium.[19] In catalytic chemistry, the trisoxazoline scandium complex [Sc(*i*Pr-trisox)(CH_2SiMe_3)$_3$] {trisox = 1,1,1-tris(oxazolinyl)methane} reported by Gade showed exceptional reactivity in α-olefin polymerisation only when two equivalents of activator were used, observations that were later used to expand the scope to less thermally stable paramagnetic lanthanide derivatives.[20] These examples illustrate that a deeper understanding of the coordination and organometallic chemistry of scandium is warranted, in order to probe reactivity trends and to provide a greater understanding of rare-earth organometallic chemistry in general.

Scandium complexes bearing chiral oxazoline-derived ligands have found widespread use in Lewis acid catalysis, with significant advances in asymmetric synthesis being developed in the groups of Evans[21] and others.[11] Besides the afore-mentioned α-olefin polymerisation catalysts, and the butadiene polymerisation catalysts reported by Li et al.,[22] there are few reports of oxazoline-supported organometallic-type (i.e. complexes including highly basic co-ligands such as alkyl, hydride, and amide) scandium complexes, and a thorough investigation of their coordination and reaction chemistry has not been forthcoming.

One of the obstacles that hinder the use of oxazoline ligands in such complexes is the propensity of the oxazoline moiety to undergo ring-opening decomposition reactions in the presence

[a] *School of Chemistry, Cardiff University, Main Building, Park Place, Cardiff CF10 3AT, UK*
E-mail: WardBD@Cardiff.ac.uk
http://www.cardiff.ac.uk/people/view/38527-ward-benjamin

Supporting information and ORCID(s) from the author(s) for this article are available on the WWW under http://dx.doi.org/10.1002/ejic.201600223.

of nucleophilic co-ligands. This phenomenon may be exemplified by considering the Group 4 coordination chemistry of 2-amino-oxazoline ligands, in which titanium and zirconium amido complexes were found to undergo ring-opening, affording amido-alkoxide derivatives.[23,24] Whilst this type of side-reaction has been rarely characterised in as much detail, it is reasonable to suggest that they may be more widely responsible for catalyst degradation in early transition-metal and lanthanide-catalysed reactions in which oxazoline-derived ligands are employed alongside highly nucleophilic co-ligands.

As part of our ongoing investigation into the coordination chemistry and reactivity of rare-earth complexes bearing oxazoline ligands, we have recently reported on the use of the bis(oxazolinylphenyl)amide (BOPA) ligands[25] to support alkyl- and amido rare-earth complexes. Our studies probed the photophysical properties of paramagnetic lanthanide complexes, their use in hydroamination/cyclisation catalysis, and in the ring-opening polymerisation of *rac*-lactide.[26] In this contribution, we report on the coordination chemistry and properties of scandium complexes bearing the BOPA ligand, including alkyl, chloride, and amido derivatives – our purpose being to provide a deeper understanding into the coordination chemistry of rare-earth complexes bearing oxazoline ligands and to explore the scope and limitations of their stoichiometric reaction chemistry.

Results and Discussion

Synthesis of [Sc{N(SiMe$_3$)$_2$}$_2$Cl(THF)] (1)

We have previously demonstrated that the homoleptic lanthanide amide complexes, [Ln{N(SiMe$_3$)$_2$}$_3$] (Ln = Y, La, Sm, Pr, Nd), are suitable precursors for the preparation of lanthanide BOPA complexes.[26] We therefore initially sought to prepare scandium derivatives using [Sc{N(SiMe$_3$)$_2$}$_3$]. However, despite using forcing conditions (110 °C in toluene), reactions of [Sc{N(SiMe$_3$)$_2$}$_3$] with the R-BOPA protio-ligands did not effect any reaction. NMR tube scale reactions in C_6D_6 allowed the reactions to be monitored in situ; in each case the spectra indicated the presence of unreacted starting materials. Since scandium possesses a significantly smaller ionic radius than the other rare-earth metals, we attributed this lack of reactivity to unacceptably high activation energies as a result of steric crowding of the scandium centre. This is congruous with our previous observations, in which the yttrium analogue required heating to effect the preparation of [Y(R-BOPA){N(SiMe$_3$)$_2$}$_2$].[26b] We resolved this impasse by preparing an alternative precursor, [Sc{N(SiMe$_3$)$_2$}$_2$Cl(THF)] (**1**). Several f-block derivatives of [Ln{N(SiMe$_3$)$_2$}$_2$Cl(THF)] (Ln = Pr,[27] Sm,[28] Nd[29]) have been prepared by the reaction of [Ln{N(SiMe$_3$)$_2$}$_3$] with $LnCl_3$, although the europium congener has been found to be unstable.[30] However, to the best of our knowledge there is only a single patent reference to the scandium variant,[31] and it has not been used to study the coordination chemistry of scandium.

[Sc{N(SiMe$_3$)$_2$}$_2$Cl(THF)] (**1**) was prepared by the reaction of a THF suspension of $ScCl_3(THF)_3$ with exactly *two* molar equivalents of LiN(SiMe$_3$)$_2$ (Scheme 1). The ^{1}H and ^{13}C{^{1}H} NMR spectra were consistent with a single product; there were no signals corresponding to any redistribution products, including [Sc{N(SiMe$_3$)$_2$}$_3$] (spectra were compared to independently prepared samples of this material). The reaction of intermediate quantities of LiN(SiMe$_3$)$_2$ (e.g. 2.5 equiv.) with $ScCl_3(THF)_3$ resulted in mixtures containing only **1** and [Sc{N(SiMe$_3$)$_2$}$_3$]. Interestingly, when $YCl_3(THF)_{3.5}$ was treated with two equivalents of LiN(SiMe$_3$)$_2$, only [Y{N(SiMe$_3$)$_2$}$_3$] and unreacted $YCl_3(THF)_{3.5}$ were isolated. The molecular structure of **1** was confirmed by single-crystal X-ray diffraction; the molecular structure is depicted in Figure 1, and selected metric parameters are provided in Table 1.

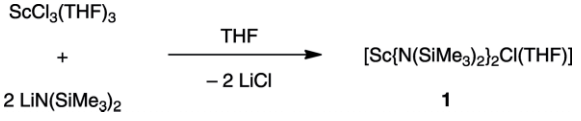

Scheme 1. Preparation of [Sc{N(SiMe$_3$)$_2$}$_2$Cl(THF)] (**1**).

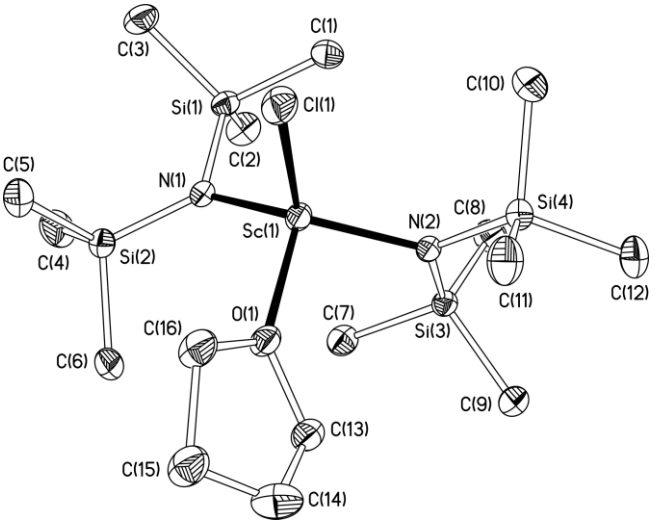

Figure 1. Molecular structure of [Sc{N(SiMe$_3$)$_2$}$_2$Cl(THF)] (**1**), displacement ellipsoids are drawn at 30 % probability. Only one disordered THF component is shown, and H atoms have been omitted for clarity.

Table 1. Selected bond lengths [Å] and angles [°] for [Sc{N(SiMe$_3$)$_2$}$_2$Cl(THF)] (**1**).

Sc(1)–N(1)	2.040(3)	Sc(1)–O(1)	2.126(3)
Sc(1)–N(2)	2.052(3)	Sc(1)–Cl(1)	2.3788(15)
Cl(1)–Sc(1)–N(1)	108.24(9)	N(1)–Sc(1)–N(2)	125.94(12)
Cl(1)–Sc(1)–N(2)	114.66(10)	N(1)–Sc(1)–O(1)	109.51(12)
Cl(1)–Sc(1)–O(1)	95.60(8)	N(2)–Sc(1)–O(1)	97.64(11)

The scandium adopts a four-coordinate geometry and is best described as a distorted tetrahedron, as there is significant deviation from the ideal 109.5° in the angles subtended at scandium. A comparison with Sc–N_{amide}, Sc–Cl, and Sc–O_{THF} distances found within the Cambridge Structural Database indicates that the scandium-ligand bond lengths are within the expected ranges (Sc–N_{amide} = 1.943–2.621, mean 2.116 Å; Sc–Cl = 2.326–2.562, mean 2.417 Å; Sc–O_{THF} = 2.116–2.378, mean 2.203 Å).[32]

The two nitrogen atoms possess trigonal planar geometries [sum of angles subtended at N(1): 358.41(48)°; at N(2): 360.0(48)°], which shows that they can, in principle, act as anionic three-electron donors through both σ and p_π interactions. The bonding in **1** was evaluated using DFT/NBO calculations. An analysis of the NBOs indicates that the two highest occupied orbitals correspond to p-based lone pairs on the N_{amido} atoms (Figure 2), thus suggesting that the amido p_π interaction with scandium is minimal in this case.

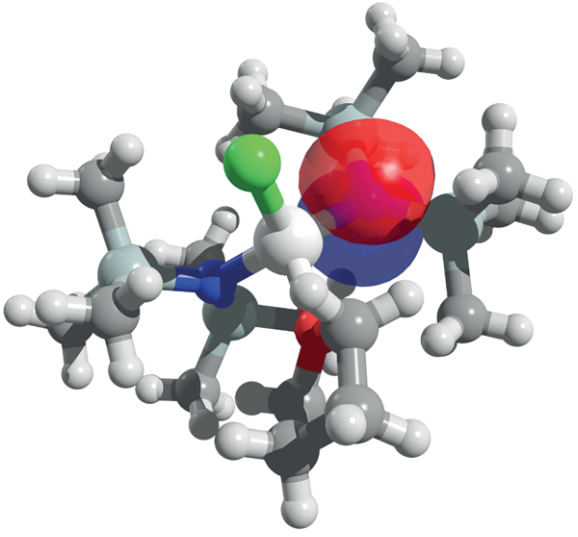

Figure 2. Calculated structure of [ScCl{N(SiMe$_3$)$_2$}$_2$(THF)] (**1**) showing the highest occupied NBO [B3LYP/SDD-6-31G(d,p)].

Synthesis of BOPA Complexes

Although the R-BOPA protio-ligands failed to react with [Sc{N(SiMe$_3$)$_2$}$_3$], the corresponding reaction with [Sc{N(SiMe$_3$)$_2$}$_2$Cl(THF)] (**1**), upon moderate heating, afforded the mixed amido-chloride complexes [Sc(R-BOPA){N(SiMe$_3$)$_2$}Cl] [R = *i*Pr (**2a**), Ph (**2b**), Bn (**2c**)] (Scheme 2). The ^{1}H and ^{13}C{^{1}H} NMR spectra were consistent with a C_1-symmetric species, as expected in a complex bearing two non-identical co-ligands. Interestingly, the N(SiMe$_3$)$_2$ co-ligands were observed, in both the ^{1}H and ^{13}C{^{1}H} NMR spectra, as *two* singlets, integrating to 9 H each. This is somewhat unusual, since such ligands are commonly observed as one singlet of 18 H relative intensity.[26] Whilst the observation of formally inequivalent SiMe$_3$ groups is readily understood in such an asymmetric complex, one would normally expect them to be rapidly interconverting through rotation of the Sc–N bond; the fact that this is not observed in **2a**–**c** highlights the extreme steric crowding that the BOPA ligand exerts to suppress this rotation altogether.

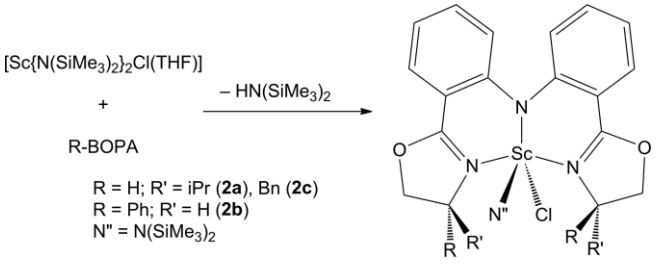

Scheme 2. Preparation of [Sc(R-BOPA){N(SiMe$_3$)$_2$}Cl] (**2**).

Each of the complexes **2a**–**c** (and all of the BOPA complexes reported in this article) exists in two isomeric forms (Figure 3). Both species were evident in the ^{1}H and ^{13}C{^{1}H} NMR spectra, but the two isomers could not be isolated independently. Analysis of the mixtures using spin saturation transfer (SST) NMR experiments indicated that the two isomers were exchanging on a chemical timescale, and further 2D NMR experiments (HSQC and HMBC) established that the two isomers possess identical connectivities. We therefore attribute the two isomers to those possessing differing helical twists in the diphenylamide backbone, denoted *exo* and *endo* on the basis of the relative orientation of the stereodirecting groups, as discussed in our previous reports. Further evidence for our conclusion is provided by the solid-state structure of [Sc(*i*Pr-BOPA)(CH$_2$SiMe$_3$)$_2$] reported by Li et al.;[22] an inspection of the structure reveals that this complex crystallises in the opposite isomer to the neodymium and samarium structures provided in our previous work.[26] For these scandium complexes, the exchange process is clearly much slower than that observed for the larger rare-earth metals, since in our previous report only the yttrium complexes showed this behaviour by NMR spectroscopy; for the metals with larger ionic radii, the isomers were only detected using luminescence spectroscopy. This observation suggests that the ionic radius of the metal has an influence of the rate of isomer interchange, possibly owing to the respective M–L distances; shorter M–L distances lead to greater steric interactions within the ligand manifold, thus reducing the rate of exchange. Whilst we have reported on these equilibria for the other rare-earth complexes, we have not thoroughly investigated them owing to the limited data available. The slower rate of exchange in these scandium complexes means that we are now able to report more fully on this matter, as discussed below.

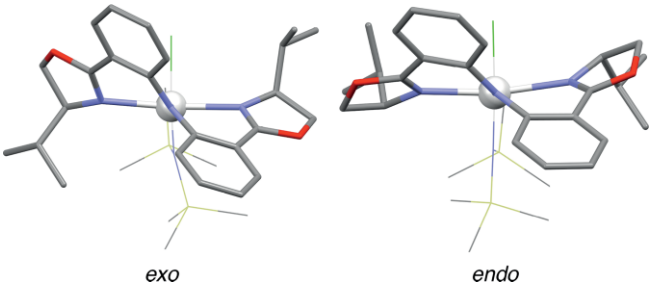

Figure 3. *exo* and *endo* isomers of [Sc(*i*Pr-BOPA){N(SiMe$_3$)$_2$}Cl] (**2a**).

Complexes **2a**–**c** have the potential for independently reacting either the amide or the chloride co-ligand without affecting the other. To this end, we probed each of these scenarios in turn using reaction strategies that are common for each category of co-ligand.

Reaction of [Sc(R-BOPA){N(SiMe$_3$)$_2$}Cl] (**2a**–**c**) with silver triflate in toluene afforded a white precipitate (silver chloride). The complexes [Sc(R-BOPA){N(SiMe$_3$)$_2$}(OTf)] [R = *i*Pr (**3a**), Ph (**3b**), Bn (**3c**)] were isolated as yellow/green, air- and moisture sensitive

complexes, the result of selectively abstracting the chloride ligands from the scandium (Scheme 3). In contrast to **2a**–**c**, the ^{1}H and $^{13}C\{^{1}H\}$ NMR spectroscopic data are consistent with C_2-symmetric species, with modest differences in all chemical shifts compared to those in the amido-chloride precursors. Both *exo* and *endo* isomers were evident from these spectra. Most notably, the $N(SiMe_3)_2$ resonances were observed as a single signal, which is again a significant difference to the spectra of **2**. On the basis of these data, we could hypothesise (reasonably) that the triflate anions are non-coordinating, and that the scandium complexes **3a**–**c** exist as cationic species; however a closer analysis of the $^{13}C\{^{1}H\}$ and ^{19}F NMR spectra indicate that there are *two* signals attributed to the triflate anion, for the *exo* and *endo* isomers, respectively (and at a different chemical shift to silver triflate in C_6D_6; –76.9 ppm, compared to –77.8 and –78.1 for **3b**). These data are consistent with significant interaction between the scandium and triflate under the conditions of the spectroscopic measurements, and hence the reason we include the triflate ion in the inner coordination sphere throughout this account.

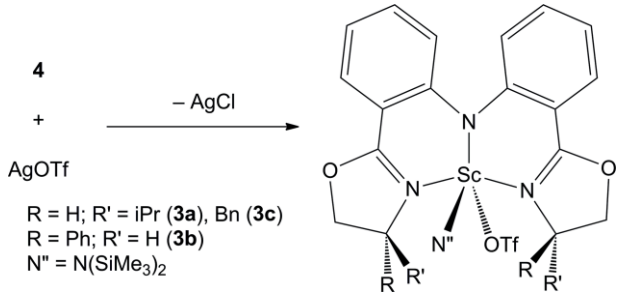

Scheme 3. Preparation of [Sc(R-BOPA){$N(SiMe_3)_2$}(OTf)] (**3**).

Having demonstrated that the chloride ligand can be abstracted, we explored the reactivity of the bis(trimethylsilyl)-amide ligand, by reacting [Sc(R-BOPA){$N(SiMe_3)_2$}Cl] (**2a**–**c**) with *para*-cresol (Scheme 4). These reactions were performed on an NMR tube scale in C_6D_6, and in each case the ^{1}H NMR spectra showed that the products were contaminated by appreciable quantities of R-BOPA protio-ligand. Nevertheless, the remaining signals were consistent with the *para*-cresol having protonated the scandium amide ligand and with the formation of the corresponding aryloxide complexes [Sc(R-BOPA)Cl(O-4-C_6H_4Me)] [R = *i*Pr (**4a**), Ph (**4b**), Bn (**4c**)]. Evidence for their formation was also provided by signals attributed to $HN(SiMe_3)_2$, which could be removed under reduced pressure, and by signals consistent with a coordinated 4-*O*-C_6H_4Me moiety, with signals at slightly different chemical shifts to those of *para*-cresol in C_6D_6. The complexes **4a**–**c** were observed as *exo* and *endo* isomers; due to the presence of two isomers in addition to the protio-ligand, some of the NMR signals were overlapping (particularly for the phenyl and benzyl derivatives with a large number of aromatic signals), but sufficient confidence in their assignment was obtained by employing a range of 2D NMR experiments, including COSY, HSQC, and HMBC. Scale-up reactions gave products with identical NMR spectra, but samples could not be separated from persistent traces of the protio-ligand, which were consistently observed as contaminants after repeated recrystallisations. An expansion of the ^{1}H NMR spectrum of **4b** is shown in Figure 4, highlighting the signals attributed to the major and minor isomers, as well as those corresponding to the protio-ligand (superimposed for clarity). Therefore characterising data for these complexes were limited to ^{1}H and $^{13}C\{^{1}H\}$ NMR spectra.

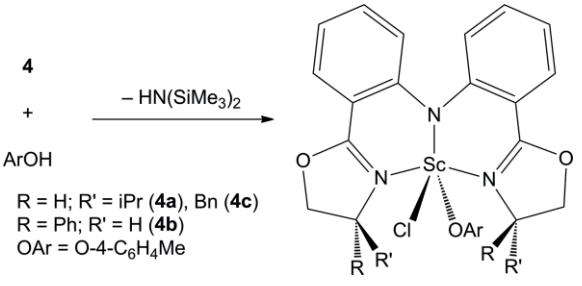

Scheme 4. Preparation of [Sc(R-BOPA)Cl(O-4-C_6H_4Me)] (**4**).

The structures of complexes **2**, **3**, and **5** (vide infra) were calculated using the B3LYP hybrid DFT functional, which is routinely employed for coordination complexes and gives reliable data. In each case, the highest occupied molecular orbitals were found to contain a significant density on the amido nitrogen of the BOPA ligand. The two highest occupied orbitals taken from a Natural Bonding Orbital analysis of [Sc(Ph-BOPA){$N(SiMe_3)_2$}Cl]

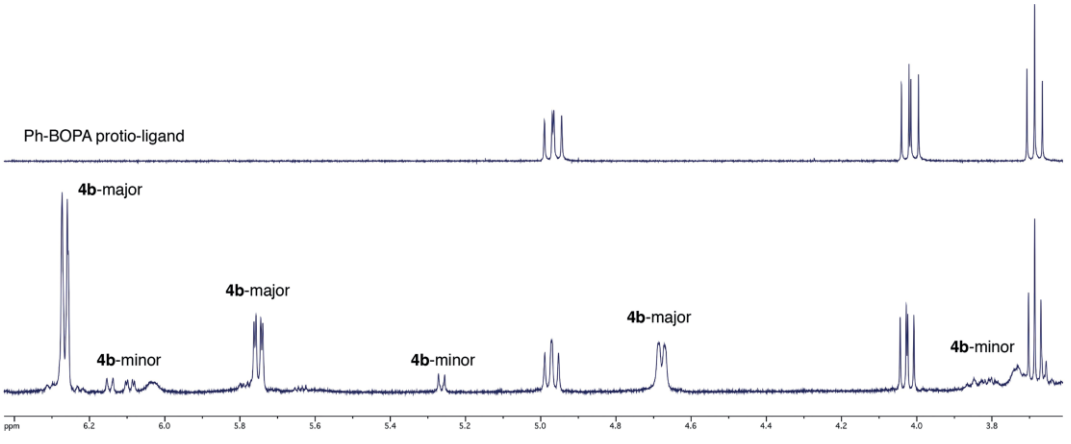

Figure 4. ^{1}H NMR sub-spectra (500 MHz, C_6D_6, 293 K) of [Sc(Ph-BOPA)Cl(*O*-4-C_6H_4Me)] (**4b**) and the Ph-BOPA protio-ligand.

(**2b**) are shown in Figure 5. These orbitals are associated with the non-bonding electron pair of the $N(SiMe_3)_2$ nitrogen atom and the amido nitrogen atom of the BOPA ligand.

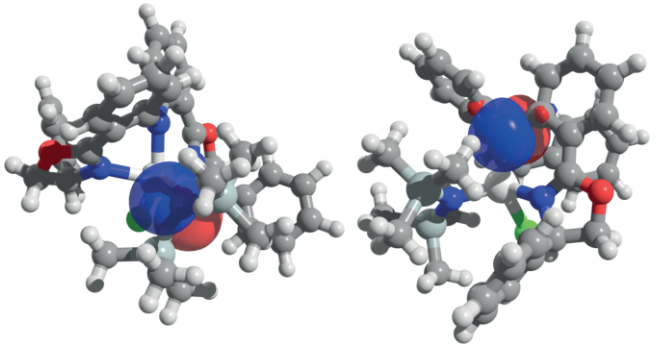

Figure 5. The two highest occupied NBOs for [Sc(Ph-BOPA){$N(SiMe_3)_2$}Cl] (**2b**) [B3LYP/SDD-6-31G(d,p)].

The amido $[NR_2]^-$ ligand can be considered as being either a 1- or 3-electron donor. In early-transition-metal complexes, they are usually regarded as 3-electron donors, involving both σ and $p_\pi \rightarrow d_\pi$ interactions.[33] However there have been cases where there are more p_π donors than d_π acceptors ("π-loaded" complexes), thus making nitrogen-based p_π electrons effectively non-bonding.[34] Such a situation has been shown to have a pronounced effect on their subsequent reactivity, rendering the M–NR_2 moiety subject to protonation and insertion reactions.[35] Although these BOPA complexes are not π-loaded, the calculations suggest that there is little, if any, $p_\pi \rightarrow d_\pi$ bonding with the scandium-bound amides. Therefore any protonation-type reaction involving these complexes is likely to lead to competing reactions, in which both the monodentate co-ligands and the BOPA ligands can be protonated under identical experimental conditions, giving mixtures of products, consistent with our experimental observations.

Zhang, Li and co-workers have demonstrated that the *i*Pr-BOPA protio-ligand reacts with the organometallic precursors $[Ln(CH_2SiMe_3)_3(THF)_2]$ (Ln = Sc, Y, Lu, Tm). Whilst rare-earth elements with larger ionic radii (Y and Tm) underwent ring-opening of the oxazoline rings, those with smaller ionic radii (Sc and Lu) formed well-defined stable complexes that were active in the polymerisation of isoprene.[22] We sought to extend the knowledge-base of analogous organometallic complexes by using the full range of BOPA ligand derivatives included in this article, but bearing the alternative alkyl ligand, CH_2SiMe_2Ph. This ligand, first reported by Piers et al., has been used much less as a Group 3/lanthanide co-ligand, but has the advantage of being significantly more thermally robust than CH_2SiMe_3.[36] We have successfully prepared yttrium complexes bearing this alkyl ligand and found them to be thermally stable.[26b]

The alkyl precursor $[Sc(CH_2SiMe_2Ph)_3(THF)_2]$ reacts cleanly with the three BOPA protio-ligands R-BOPA to afford the dialkyl complexes [Sc(R-BOPA)$(CH_2SiMe_2Ph)_2$] [R = *i*Pr (**5a**), Ph (**5b**), Bn (**5c**)] with the concomitant elimination of phenyltrimethylsilane (Scheme 5). The complexes were afforded as air-sensitive yellow solids, but other than their instantaneous reaction with air/water (evidenced by rapid discoloration of the solid on contact with air and the protio-ligand being observed by ^{1}H NMR spectroscopy), the complexes were remarkably stable to heat; after heating solutions of **5a**–**c** to 80 °C in C_6D_6 for 24 h there was no evidence of thermal decomposition, either by the often observed elimination of alkane (appearance of a signal attributed to $PhSiMe_3$)[37] or by ring-opening of the oxazoline rings. As with all of the five-coordinate complexes reported in this article, **5a**–**c** were observed in two isomeric forms.

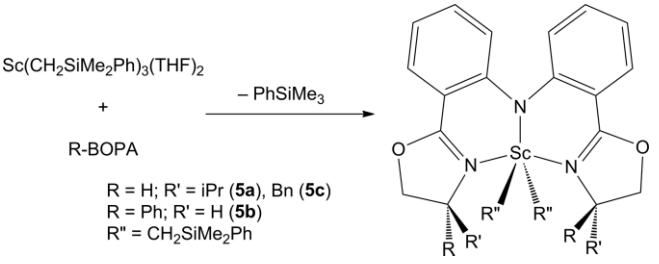

Scheme 5. Preparation of [Sc(R-BOPA)$(CH_2SiMe_2Ph)_2$] (**5**).

Equilibrium Analyses

We examined the thermodynamics of the equilibria using variable temperature NMR spectroscopy, allowing us to validate our hypothesis relating to the isomeric forms. We chose to study [Sc(*i*Pr-BOPA){$N(SiMe_3)_2$}Cl] (**2a**) as a representative example. The equilibrium position was determined by integration of ^{1}H NMR spectra measured between –5 and +65 °C. These data were used to construct a van 't Hoff plot (Figure 6), from which the enthalpy and entropy of the equilibrium were extracted to give $\Delta H^0 = 5.2 \pm 1$ kJ mol^{-1} and $\Delta S^0 = 1.1 \pm 3$ J mol^{-1} K^{-1}. The value of ΔS^0 is sufficiently close to zero to be consistent with no alteration in denticity of the supporting ligand. These parameters have allowed us to estimate the value of ΔG^0_{298} to be 4.9 ± 1.5 kJ mol^{-1}, which is in good agreement with the value obtained using DFT calculations (vide infra).

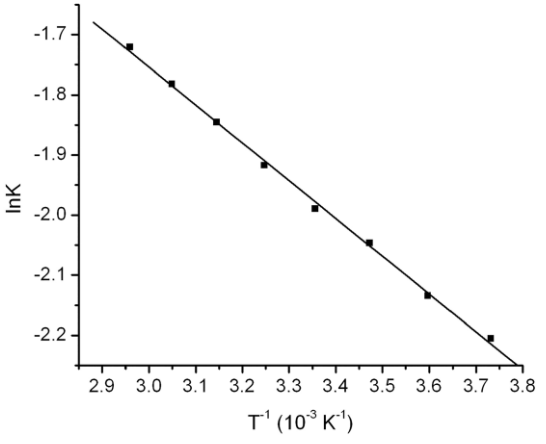

Figure 6. van 't Hoff plot for the *exo*–*endo* equilibrium of [Sc(*i*Pr-BOPA){$N(SiMe_3)_2$}Cl] (**2a**).

The thermodynamic studies were supplemented by computational analyses. The two isomers of the scandium BOPA complexes are energetically similar (<5 kJ mol^{-1}); such energy differences are at the limit of computational accuracy, which is typically 2–3 kcal mol^{-1} (8–12 kJ mol^{-1}). Nevertheless, the relative

energies of the *endo* and *exo* isomers of **2**, **3** and **5** were calculated and are provided in Table 2, along with energies calculated from the equilibrium coefficients measured at 298 K.

Table 2. Relative energies (calculated and experimental) for scandium BOPA complexes [B3LYP/SDD-6-31G(d,p)].

Complex		R	ΔG_{exp}[a]	ΔG_{DFT}[a,b]
[Sc(R-BOPA){N(SiMe$_3$)$_2$}Cl]	**2a**	*i*Pr	3.6	–4.2
	2b	Ph	3.9	20.0
	2c	Bn	0.9	6.7
[Sc(R-BOPA){N(SiMe$_3$)$_2$}(OTf)]	**3a**	*i*Pr	1.7	–7.9
	3b	Ph	2.2	10.0
	3c	Bn	1.2	13.1
[Sc(R-BOPA)(CH$_2$SiMe$_2$Ph)$_2$]	**5a**	*i*Pr	1.7	–8.4
	5b	Ph	1.7	–4.9
	5c	Bn	1.2	8.1

[a] kJ mol^{-1}. [b] $G_{endo} - G_{exo}$.

The mean deviation of (absolute) experimental and calculated energies is 8.6 kJ mol^{-1}, which is reasonable, given the accepted error associated with such calculations (vide supra). The energies in Table 2 were calculated with the formula $E_{endo} - E_{exo}$; negative values therefore suggest that the *endo* isomer is more stable. For consistency, the experimental values are calculated from I_{major}/I_{minor}, and no inference as to whether the *exo* or *endo* isomer constitutes the major isomer is suggested by these data alone. Nevertheless, our previous studies of paramagnetic species strongly suggest that the major species is the *exo* isomer; the majority of these calculations are consistent with this proposition. These calculations suggest that the two isomers have small energy differences, regardless of stereodirecting group or co-ligand, and are therefore consistent with experimental observations made using NMR spectroscopy. The precise factors governing which is the more stable isomer are likely to be dominated by steric effects, which arise from repulsion between the two stereodirecting groups (which are in closer proximity for the *endo* isomer) and the co-ligands, which will vary as a function of not only their size, but also rigidity of the groups [e.g. CH$_2$SiMe$_2$Ph vs. N(SiMe$_3$)$_2$].

Transition states for the interchange of the *exo* and *endo* isomers could not be located for any of the complexes described experimentally, possibly due to the relatively large numbers of degrees of freedom in the co-ligands. Therefore, a model complex was calculated, [Sc(*i*Pr-BOPA)Me$_2$] (**6**$_{calc}$), reducing conformational flexibility by using methyl co-ligands. The transition state corresponding to a concerted exchange of the *exo* and *endo* isomers, TS-**6**$_{calc}$, was located and suggests a high activation energy (ΔH_{calc} = 96 kJ mol^{-1}; ΔG_{calc} = 102 kJ mol^{-1} relative to *exo*-**6**$_{calc}$, Figure 7), consistent with the experimental observations since high temperature NMR spectroscopy failed to cause coalescence. For comparative purposes, the experimentally determined activation barrier for the rotation of a 2,6-dimethylphenyl group in a tungsten imido complex reported by Mountford, Gade and co-workers was found to be 77 kJ mol^{-1}, and in this case line broadening was observed only at +50 °C.[38] It is therefore understandable that the activation barrier in these BOPA complexes should be somewhat higher. The *endo* isomer was found to be slightly endothermic (ΔH_{calc} = +12 kJ mol^{-1}; ΔG_{calc} = 15 kJ mol^{-1}) relative to *exo*-**6**$_{calc}$, consistent with the *exo* isomer being the major component of these complexes.

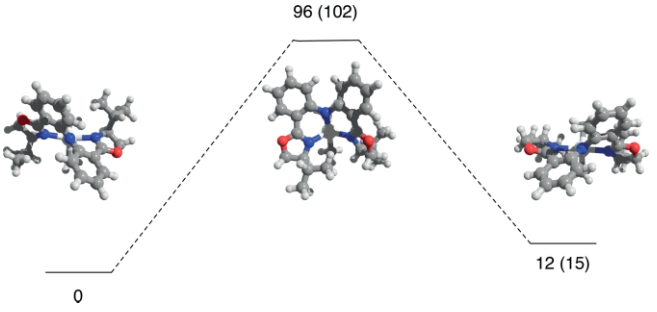

Figure 7. Calculated (B3LYP/SDD-6-31G(d,p)) relative enthalpies (free energies) for the interchange of *exo* and *endo* isomers of [Sc(*i*Pr-BOPA)Me$_2$] (**6**$_{calc}$) (kJ mol^{-1}).

The calculated structure TS-**6**$_{calc}$ is displayed in Figure 8. In comparison to *exo*-**6**$_{calc}$ and *endo*-**6**$_{calc}$, the BOPA ligand adopts a highly distorted coordination motif, necessary for the two phenyl rings to pass. The Sc–N$_{amide}$ bond is significantly lengthened to 2.328 Å (cf. 2.207 and 2.163 Å in *exo*-**6**$_{calc}$ and *endo*-**6**$_{calc}$, respectively), although the N$_{amide}$ itself remains approximately sp^2 hybridised – the sum of angles subtended is 356.9° and therefore not significantly deviating from 360°. Most noticeable is the arrangement of oxazoline and methyl donors: The N$_{oxazoline}$–Sc–N$_{oxazoline}$ was calculated as 156.1 and 165.1° in *exo*-**6**$_{calc}$ and *endo*-**6**$_{calc}$, whereas in TS-**6**$_{calc}$ this angle is more acute, at 111.1°. Moreover, the methyl groups in TS-**6**$_{calc}$ were found in two distinct environments, with corresponding N$_{amide}$–Sc–C angles of 167.4 and 92.7°. The equivalent angles in the ground state structures were 118.2 and 133.1° (*exo*-**6**$_{calc}$), and 119.8 and 117.5° (*endo*-**6**$_{calc}$).

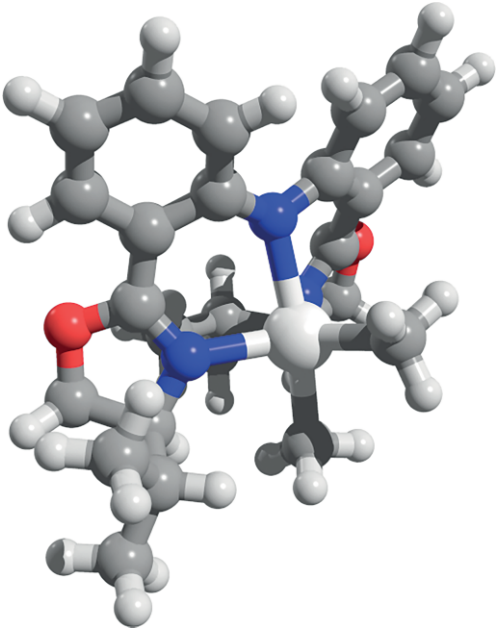

Figure 8. Calculated (B3LYP/SDD-6-31G(d,p)) transition-state structure for the interconversion of *exo* and *endo* isomers of [Sc(*i*Pr-BOPA)Me$_2$] (**6**$_{calc}$).

For completeness, a dissociative mechanism for the interchange of isomers was calculated. This mechanism proposes the de-coordination of one oxazoline donor, followed by the rotation of the N_{amide}–Ar bond. The calculations suggest that the de-coordination of an oxazoline is endergonic by 99 kJ mol^{-1}. Subsequent rotation of the N_{amide}–Ar bond gives a total activation energy of 168 kJ mol^{-1}. The energy profile for this mechanism is provided in the Supporting Information, Figure S2.1. Our overall conclusion from these calculations is that the concerted exchange process is credible, whereas the dissociative pathway is improbable.

Spectroscopic Properties

The photophysical properties of [Sc(R-BOPA){N(SiMe$_3$)$_2$}Cl] (**2a**–**c**) and [Sc(R-BOPA)(CH$_2$SiMe$_2$Ph)$_2$] (**5a**–**c**) (in dry benzene, 10^{-4} M under N_2 atmosphere) were investigated;[39] the emission profiles are provided in Figure 9. The complexes show a single emission peak between (493–522 nm) following excitation at 485 nm (Table 3), with a small associated Stokes' shift (ca. 1000 cm^{-1}); the precise positioning of the emission showed a small dependence on the specific identity of the BOPA ligand. The diphenylamine anion is known to be non-emissive,[40] and therefore the fluorescence from these complexes is attributed to a ligand-centred excited state with a significant charge transfer (N→π*) component originating from the deprotonated/coordinated amide bridge-head.

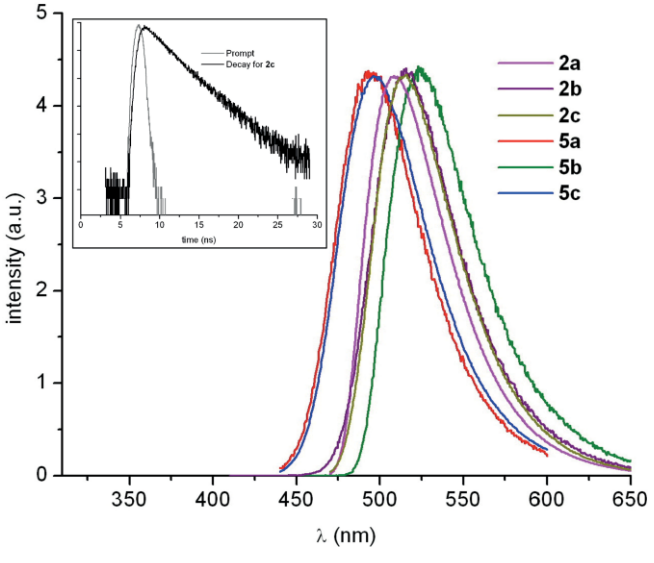

Figure 9. Main: normalised emission profiles (λ_{ex} = 485 nm) of [Sc(R-BOPA){N(SiMe$_3$)$_2$}Cl] (**2a**–**c**) and [Sc(R-BOPA)(CH$_2$SiMe$_2$Ph)$_2$] (**5a**–**c**). Inset: time-resolved decay profile for **2c**.

The lifetimes (Table 3) are short (< 10 ns) and consistent with a ligand-centred fluorescence. As with our previous studies on paramagnetic lanthanide BOPA complexes,[26] the decay profiles were best-fit to a biexponential function yielding two distinct lifetime values. This observation indicates the presence of two components, which could be attributed to the *exo* and *endo* isomers, as observed in the ^{1}H NMR spectra.

Table 3. Emission wavelengths and lifetimes of [Sc(R-BOPA){N(SiMe$_3$)$_2$}Cl] (**2a**–**c**) and [Sc(R-BOPA)(CH$_2$SiMe$_2$Ph)$_2$] (**5a**–**c**) (benzene, N_2).

Entry	Complex	Emission, λ_{em} / nm[a]	Lifetime, τ / ns[b]
1	**2a**	506	2.3, 3.7 (82 %)
2	**2b**	512	2.0, 3.6 (89 %)
3	**2c**	511	2.8, 4.5 (53 %)
4	**5a**	493	1.5, 3.6 (41 %)
5	**5b**	522	0.8, 3.2 (59 %)
6	**5c**	494	1.3, 3.3 (51 %)

[a] λ_{ex} = 485 nm. [b] λ_{ex} = 459 nm, λ_{em} = 505 nm.

Insight into the spectroscopic properties was obtained using TD-DFT calculations. As a representative example, the first 24 excited states calculated for *exo*-[Sc(Ph-BOPA){N(SiMe$_3$)$_2$}Cl] *exo*-**2b** are depicted alongside a simulated spectrum in Figure 10 (with the experimental UV/Vis spectrum superimposed). Tabulated summaries of all TD-DFT calculated excited states are provided in the Supporting Information.

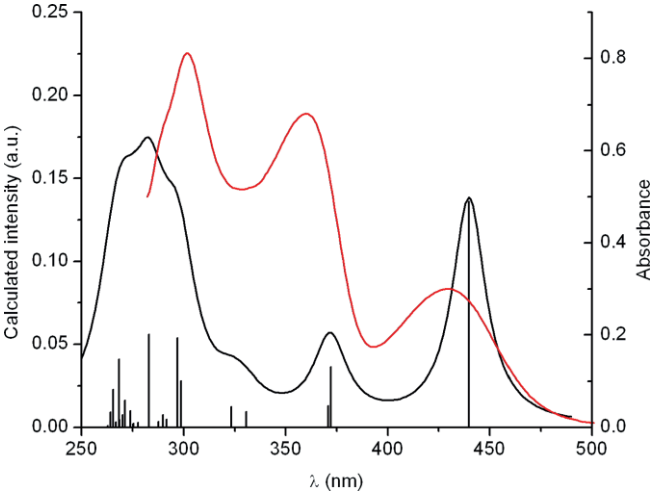

Figure 10. Simulated (black) and experimental (red, 10^{-4} M, toluene) absorption spectra for [Sc(Ph-BOPA){N(SiMe$_3$)$_2$}Cl] (**2b**) using TD-DFT data. The vertical lines indicate the individual excited state components.

Since each complex contains both *exo* and *endo* components concurrently, the simulated spectrum of an individual component is not expected to accurately resemble an experimental spectrum, even though the calculated spectra for the *exo* and *endo* isomers are similar for any given complex. It is therefore inappropriate to closely compare relative intensities and energies of observed and calculated maxima. Nevertheless, an analysis of the TD-DFT output shows that the excited states are dominated by π→π* and n→π*, involving the non-bonding amide p_π lone pairs and, to a lesser extent, the chloride lone pairs. The lowest calculated energy excitation at 440 nm correlates quite well with the observed excitation band, which appears as a sharp peak around 470 nm and is attributed to significant n→π* character. Most notable is the relatively large number of transitions at <400 nm, which gives rise to a rather poorly defined spectral profile, as observed in the experimental excitation spectra depicted in Figure S3.1 (Supporting Information). The TD-DFT data for the *endo* isomer, and those for the other complexes studied, are also consistent with this observation.

Conclusions

We have investigated the coordination chemistry of scandium supported by BOPA ligands; we find that the BOPA ligands support a range of complexes bearing several classes of co-ligand, and we find no evidence of ring-opening of the oxazoline ligands. In particular, we have shown that non-symmetrical amido-chloride complexes can be prepared using $[Sc\{N(SiMe_3)_2\}_2Cl(THF)]$ (**1**), a useful precursor that has not previously been used in the coordination chemistry of scandium. We have established the scope and limitations of the stoichiometric reaction chemistry of these complexes, in that the amido and chloride ligands can be reacted independently, but there are limitations when the supporting ligand contains an amide moiety that can undergo competitive protonation (as the BOPA ligand does in this case). We have demonstrated that these complexes exist as two isomers, and our data suggest that a concerted pathway is the most likely mechanism for interconversion.

On the basis of our studies, particularly the stoichiometric reaction chemistry, we propose that oxazoline-containing ligands have much to offer in regard to supporting organometallic-type rare-earth complexes, and that there is the potential for such complexes to find a greater application in catalytic transformations.

Experimental Section

General Methods and Instrumentation: All manipulations of air- and moisture-sensitive species were performed under an atmosphere of argon or dinitrogen using standard Schlenk and glove box techniques. Solvents were dried by passing through an alumina drying column incorporated into a MBraun SPS800 solvent purification system, except for tetrahydrofuran, which was dried with molten potassium for three days and distilled under argon. All solvents were degassed, saturated with argon, and stored under argon in Teflon valve ampoules prior to use. Deuterated solvents for NMR spectroscopy were dried with molten potassium ($[D_6]$benzene, $[D_8]$toluene) for three days before being vacuum transferred, freeze-pump-thaw degassed and stored in a glove box. $CDCl_3$ for non-sensitive samples was passed through a column of basic alumina before being stored over 4 Å molecular sieves prior to use. $LiN(SiMe_3)_2$,[41] $[Sc(CH_2SiMe_2Ph)_3(THF)_2]$[36] and $[Sc\{N(SiMe_3)_2\}_3]$[42] were synthesised according to literature procedures. All other reagents were purchased from commercial suppliers and used as received unless otherwise stated.

Air-sensitive samples for NMR and luminescence spectroscopy were prepared in a glove box under a dinitrogen atmosphere using 5 mm Nolan NMR tubes equipped with J. Young Teflon valves. All other samples were prepared in Wilmad 5 mm NMR tubes. NMR spectra were recorded on Bruker Avance DPX-400 or –500 NMR spectrometers. NMR spectra are quoted in ppm relative to tetramethylsilane (δ = 0 ppm) and were referenced internally relative to the residual protio-solvent (^1H) or solvent (^{13}C) resonances; all coupling constants are quoted in Hertz. NMR assignments were confirmed by the use of two-dimensional ^1H-^1H or ^1H-^{13}C correlation experiments (HSQC and HMBC). Infrared spectra were prepared as KBr pellets and were recorded on a Jasco 660-Plus FTIR spectrometer. Infrared data are quoted in wavenumbers (cm^{-1}). All photophysical data were obtained on a Jobin Yvon-Horiba Fluorolog-3 spectrometer fitted with a JY TBX picosecond photodetection module. A Hamamatsu R5509-73 detector (cooled to –80 °C using a C9940 housing) was used for luminescence measurements. For the fluorescence lifetimes the pulsed laser source was a 459 nm NanoLEDs (operating at 1 MHz). All lifetime data were collected using the JY-Horiba FluoroHub single photon counting module in multi-channel scalar mode. Lifetimes were obtained using the provided software, DAS6. Elemental analyses were recorded by the analytical services at London Metropolitan University. Complexes **5b** and **5c** gave consistently and persistently low carbon elemental analyses despite repeated recrystallisations and giving satisfactory hydrogen and nitrogen analyses. We attribute this to incomplete combustion and carbide formation, which is a known problem for some organoscandium complexes.[43]

Crystallographic Studies: Single crystals of $[Sc\{N(SiMe_3)_2\}_2Cl(THF)]$ (**1**) suitable for X-ray analysis were grown from a saturated solution in hexanes at 5 °C overnight. X-ray data (Mo-K_α) were collected on a Rigaku Saturn 724+ CCD diffractometer at low temperature, by the EPSRC National Crystallographic Service.[44] The structure was solved by direct methods with absorption corrections being applied as part of the data reduction scaling procedure. One of the THF β-carbons (C15) was disordered over two sites. The disorder was successfully modelled giving occupancies of 0.54 and 0.46. After refinement of the heavy atoms, difference Fourier maps revealed the maxima of residual electron density close to the positions expected for the hydrogen atoms; they were introduced as fixed contributors in the structure factor calculations and treated with a riding model, with isotropic temperature factors [$U_{iso}(H) = 1.3U_{eq}(C)$] but not refined. Full least-square refinement was carried out on F^2. A final difference map revealed no significant maxima of residual electron density. Structure solution and refinement were performed using the SHELX software suite.[45] Crystal data and experimental details are provided in Table S4.1.

Density Functional Calculations: All calculations were performed on the Gaussian 09 suite.[46] Molecular geometries were optimised without symmetry restraints and were followed by frequency calculations to ascertain the nature of the stationary point (minimum vs. saddle point). Calculations were performed using the restricted B3LYP hybrid functional,[47] incorporating the D3 version of Grimme's dispersion correction.[48] The Stuttgart/Dresden basis set with *pseudo* core potentials[49] was used for Sc and 6-31G(d,p) double ζ basis set[50] for all remaining centres. Coordinates of all optimized structures are provided in the Supporting Information. NBO analyses were performed using NBO version 3, incorporated into the Gaussian program.[51] Relaxed potential energy scans were calculated by fixing the appropriate dihedral angle and allowing the structure to optimise at each value of the scanned parameter. The structure corresponding to the maximum of the potential energy surface was thereafter used as a starting geometry for a subsequent transition-state calculation using the Berny algorithm. Transition states were verified using a frequency calculation and showed a single imaginary frequency corresponding to the expected reaction coordinate. TD-DFT calculations[52] were performed using the unrestricted B3LYP functional and adding diffuse functions to the non-metal basis set, 6-31+G(d,p); the first 24 excited states were calculated in each case. As shown by Vlček et al.,[53] solvent effects can be crucial for obtaining satisfactory agreement between experiment and TD-DFT. Solvent was therefore modelled using the polarisable continuum model,[54] with the molecular cavity defined by a united atom model that incorporates hydrogen into the parent heavy atom, and included in both geometry optimisations and TD-DFT calculations. Details of all calculated excited states are provided in the Supporting Information.

Supporting Information (see footnote on the first page of this article): Experimental procedures and characterisation data, tabular summary of crystallographic parameters, all computed molecule Cartesian coordinates, summaries of excited-state calculations, and representative excitation/emission spectra are presented. The data supporting the results presented in this article are freely available via the Cardiff University Data Catalogue at http://dx.doi.org/10.17035/d.2016.0008424132 .

CCDC 1054144 (for **1**) contains the supplementary crystallographic data for this paper. These data can be obtained free of charge from The Cambridge Crystallographic Data Centre.

Acknowledgments

We thank Cardiff University (Endowment Fellowship to SDB), the Leverhulme Trust (F/00 407/BL), and the EPSRC (PhD studentship) for financial support. Access to the National Crystallographic Service[44] and the Advanced Research Computing Service at Cardiff University "ARCCA" is gratefully acknowledged.

Keywords: Scandium · Luminescence · Density functional calculations · Rare earths · Oxazoline ligands

[1] F. T. Edelmann, D. M. M. Freckmann, H. Schumann, *Chem. Rev.* **2002**, *102*, 1851.
[2] Z. Hou, Y. Wakatsuki, *Coord. Chem. Rev.* **2002**, *231*, 1.
[3] J. Gromada, J.-F. Carpentier, A. Mortreux, *Coord. Chem. Rev.* **2004**, *248*, 397.
[4] S. Hong, T. J. Marks, *Acc. Chem. Res.* **2004**, *37*, 673.
[5] S. Arndt, J. Okuda, *Adv. Synth. Catal.* **2005**, *347*, 339.
[6] G. A. Molander, J. A. C. Romero, *Chem. Rev.* **2002**, *102*, 2161.
[7] P. M. Zeimentz, S. Arndt, B. R. Elvidge, J. Okuda, *Chem. Rev.* **2006**, *106*, 2404.
[8] G. Zi, *Dalton Trans.* **2009**, 9101.
[9] M. Zimmermann, R. Anwander, *Chem. Rev.* **2010**, *110*, 6194.
[10] F. T. Edelmann, *Coord. Chem. Rev.* **2011**, *255*, 1834.
[11] B. D. Ward, L. H. Gade, *Chem. Commun.* **2012**, *48*, 10587.
[12] M. Visseaux, F. Bonnet, *Coord. Chem. Rev.* **2011**, *255*, 374.
[13] F. T. Edelmann, *Coord. Chem. Rev.* **2014**, *261*, 73.
[14] P. R. Meehan, D. R. Aris, G. R. Willey, *Coord. Chem. Rev.* **1999**, *181*, 121.
[15] S. A. Cotton, *Polyhedron* **1999**, *18*, 1691.
[16] P. Mountford, B. D. Ward, *Chem. Commun.* **2003**, 1797.
[17] Values given are for six-coordinate Ln^{3+} ions, see: R. D. Shannon, *Acta Crystallogr., Sect. A* **1976**, *32*, 751.
[18] a) E. Lu, Y. Li, Y. Chen, *Chem. Commun.* **2010**, *46*, 4469; b) E. Lu, J. Chu, Y. Chen, M. V. Borzov, G. Li, *Chem. Commun.* **2011**, *47*, 743; c) J. Chu, E. Lu, Z. Liu, Y. Chen, X. Leng, H. Song, *Angew. Chem. Int. Ed.* **2011**, *50*, 7677; *Angew. Chem.* **2011**, *123*, 7819.
[19] a) D. Schädle, C. Maichle-Mössmer, C. Schädle, R. Anwander, *Chem. Eur. J.* **2015**, *21*, 662; b) D. Schädle, M. Meermann-Zimmermann, C. Schädle, C. Maichle-Mössmer, R. Anwander, *Eur. J. Inorg. Chem.* **2015**, 1334.
[20] a) B. D. Ward, S. Bellemin-Laponnaz, L. H. Gade, *Angew. Chem. Int. Ed.* **2005**, *44*, 1668; *Angew. Chem.* **2005**, *117*, 1696; b) L. Lukešová, B. D. Ward, S. Bellemin-Laponnaz, H. Wadepohl, L. H. Gade, *Dalton Trans.* **2007**, 920; c) L. Lukešová, B. D. Ward, S. Bellemin-Laponnaz, H. Wadepohl, L. H. Gade, *Organometallics* **2007**, *26*, 4652; d) B. D. Ward, L. Lukešová, H. Wadepohl, S. Bellemin-Laponnaz, L. H. Gade, *Eur. J. Inorg. Chem.* **2009**, 866; e) X. Kang, Y. Song, Y. Luo, G. Li, Z. Hou, J. Qu, *Macromolecules* **2012**, *45*, 640.
[21] a) D. A. Evans, Z. K. Sweeney, R. Tomislav, J. S. Tedrow, *J. Am. Chem. Soc.* **2001**, *123*, 12095; b) D. A. Evans, K. A. Scheidt, K. R. Fandrick, H. W. Lam, J. Wu, *J. Am. Chem. Soc.* **2003**, *125*, 10780; c) D. A. Evans, C. E. Masse, J. Wu, *Org. Lett.* **2002**, *4*, 3375; d) D. A. Evans, J. Wu, C. E. Masse, D. W. C. MacMillan, *Org. Lett.* **2002**, *4*, 3379; e) D. A. Evans, J. Wu, *J. Am. Chem. Soc.* **2005**, *127*, 8006; f) D. A. Evans, K. R. Fandrick, H. J. Song, *J. Am. Chem. Soc.* **2005**, *127*, 8942; g) D. A. Evans, Y. Aye, J. Wu, *Org. Lett.* **2006**, *8*, 2071; h) D. A. Evans, K. R. Fandrick, *Org. Lett.* **2006**, *8*, 2249; i) D. A. Evans, K. R. Fandrick, H. J. Song, K. A. Scheidt, R. Xu, *J. Am. Chem. Soc.* **2007**, *129*, 10029.
[22] H. Liu, J. He, Z. Liu, Z. Lin, G. Du, S. Zhang, X. Li, *Macromolecules* **2013**, *46*, 3257.
[23] B. D. Ward, H. Risler, K. Weitershaus, S. Bellemin-Laponnaz, H. Wadepohl, L. H. Gade, *Inorg. Chem.* **2006**, *45*, 7777.
[24] A. L. Gott, S. R. Coles, A. J. Clarke, G. J. Clarkson, P. Scott, *Organometallics* **2007**, *26*, 136.
[25] a) H. A. McManus, P. J. Guiry, *J. Org. Chem.* **2002**, *67*, 8566; b) S.-F. Lu, D.-M. Du, S.-W. Zhang, J. Xu, *Tetrahedron: Asymmetry* **2004**, *15*, 3433; c) H. A. McManus, P. G. Cozzi, P. J. Guiry, *Adv. Synth. Catal.* **2006**, *348*, 551; d) T. Inagaki, L. T. Phong, A. Furuta, J.-I. Ito, H. Nishiyama, *Chem. Eur. J.* **2010**, *16*, 3090; e) Y. Jia, W. Yang, D.-M. Du, *Org. Biomol. Chem.* **2012**, *10*, 4739.
[26] a) S. D. Bennett, S. J. A. Pope, B. D. Ward, *Chem. Commun.* **2013**, *49*, 6072; b) S. D. Bennett, B. A. Core, M. P. Blake, S. J. A. Pope, P. Mountford, B. D. Ward, *Dalton Trans.* **2014**, *43*, 5871.
[27] E. Hemmer, C. Cavelius, V. Huch, S. Mathur, *Inorg. Chem.* **2015**, *54*, 6267.
[28] M. Karl, G. Seybert, W. Massa, S. Agarwal, A. Greiner, K. Dehnicke, *Z. Anorg. Allg. Chem.* **1999**, *625*, 1405.
[29] D. Berg, R. Gendron, *Can. J. Chem.* **2000**, *78*, 454.
[30] a) T. D. Tilley, A. Zalkin, R. A. Andersen, D. H. Templeton, *Inorg. Chem.* **1981**, *20*, 551; b) H. C. Aspinall, D. C. Bradley, M. B. Hursthouse, K. D. Sales, N. P. C. Walker, B. Hussain, *J. Chem. Soc., Dalton Trans.* **1989**, *4*, 623.
[31] N. Kei, H. Shigetaka, T. Yasuo, Japanese patent JP2008063300, March 21, 2008.
[32] D. A. Fletcher, R. F. McMeeking, D. J. Parkin, *J. Chem. Inf. Comput. Sci.* **1996**, *36*, 746 (The UK Chemical Database Service: CSD version 5.37, updated November 2015).
[33] R. A. Andersen, D. B. Beach, W. L. Jolly, *Inorg. Chem.* **1985**, *24*, 4741.
[34] A. J. Blake, P. E. Collier, L. H. Gade, P. Mountford, S. M. Pugh, M. Schubart, M. E. G. Skinner, D. J. M. Trösch, *Inorg. Chem.* **2001**, *40*, 870.
[35] a) B. D. Ward, G. Orde, E. Clot, A. R. Cowley, L. H. Gade, P. Mountford, *Organometallics* **2005**, *24*, 2368; b) B. D. Ward, G. Orde, E. Clot, A. R. Cowley, L. H. Gade, P. Mountford, *Organometallics* **2004**, *23*, 4444; c) N. Vujkovic, B. D. Ward, A. Maisse-François, H. Wadepohl, P. Mountford, L. H. Gade, *Organometallics* **2007**, *26*, 5522.
[36] a) D. J. H. Emslie, W. E. Piers, R. MacDonald, *J. Chem. Soc., Dalton Trans.* **2002**, 293; b) D. J. H. Emslie, W. E. Piers, M. Parvez, R. McDonald, *Organometallics* **2002**, *21*, 4226.
[37] Organoscandium complexes often undergo thermal decomposition to give an unidentified precipitate alongside the alkane corresponding to the alkyl group, such as that formed through α-elimination. For specific examples see: a) M. A. Putzer, G. P. Bartholomew, *Z. Anorg. Allg. Chem.* **1999**, *625*, 1777; b) ref.[43]
[38] B. D. Ward, S. R. Dubberley, L. H. Gade, P. Mountford, *Inorg. Chem.* **2003**, *42*, 4961.
[39] a) A. de Bettencourt-Dias, P. S. Barber, S. J. Bauer, *J. Am. Chem. Soc.* **2012**, *134*, 6987; b) K. Matsumoto, K. Suzuki, T. Tsukuda, T. Tsubomura, *Inorg. Chem.* **2010**, *49*, 4717; c) J. Yuasa, T. Ohno, K. Miyata, H. Tsumatori, Y. Hasegawa, T. Kawai, *J. Am. Chem. Soc.* **2011**, *133*, 9892.
[40] N. Chattopadhyay, A. Samanta, T. Kundu, M. Chowdhury, *J. Photochem. Photobiol. A* **1989**, *48*, 61.
[41] U. Wannagat, H. Niederprüm, *Chem. Ber.* **1961**, *94*, 1540.
[42] E. C. Alyea, D. C. Bradley, R. G. Copperthwaite, *J. Chem. Soc., Dalton Trans.* **1972**, 1580.
[43] B. D. Ward, A. Maisse-François, S. R. Dubberley, L. H. Gade, P. Mountford, *J. Chem. Soc., Dalton Trans.* **2002**, 2649.
[44] S. J. Coles, P. A. Gale, *Chem. Sci.* **2012**, *3*, 683.
[45] G. M. Sheldrick, *Acta Crystallogr., Sect. A* **2008**, *64*, 112.
[46] M. J. Frisch, G. W. Trucks, H. B. Schlegel, G. E. Scuseria, M. A. Robb, J. R. Cheeseman, G. Scalmani, V. Barone, B. Mennucci, G. A. Petersson, H. Nakatsuji, M. Caricato, X. Li, H. P. Hratchian, A. F. Izmaylov, J. Bloino, G. Zheng, J. L. Sonnenberg, M. Hada, M. Ehara, K. Toyota, R. Fukuda, J. Hasegawa, M. Ishida, T. Nakajima, Y. Honda, O. Kitao, H. Nakai, T. Vreven, J. A. Montgomery Jr., J. E. Peralta, F. Ogliaro, M. Bearpark, J. J. Heyd, E. Brothers, K. N. Kudin, V. N. Staroverov, R. Kobayashi, J. Normand, K. Raghavachari, A. Rendell, J. C. Burant, S. S. Iyengar, J. Tomasi, M. Cossi, N. Rega, J. M. Millam, M. Klene, J. E. Knox, J. B. Cross, V. Bakken, C. Adamo, J. Jaramillo, R. Gomperts, R. E. Stratmann, O. Yazyev, A. J. Austin, R. Cammi,

C. Pomelli, J. W. Ochterski, R. L. Martin, K. Morokuma, V. G. Zakrzewski, G. A. Voth, P. Salvador, J. J. Dannenberg, S. Dapprich, A. D. Daniels, Ö. Farkas, J. B. Foresman, J. V. Ortiz, J. Cioslowski, D. J. Fox, *Gaussian 09, Revision D.01*, Gaussian, Inc., Wallingford CT, **2010**.

[47] a) A. D. Becke, *J. Chem. Phys.* **1993**, *98*, 5648; b) C. Lee, W. Yang, R. G. Parr, *Phys. Rev. B* **1988**, *37*, 785; c) B. Miehlich, A. Savin, H. Stoll, H. Preuss, *Chem. Phys. Lett.* **1989**, *157*, 200.

[48] S. Grimme, J. Antony, S. Ehrlich, H. Krieg, *J. Chem. Phys.* **2010**, *132*, 154104.

[49] D. Andrae, U. Haeussermann, M. Dolg, H. Stoll, H. Preuss, *Theor. Chem. Acc.* **1990**, *77*, 123.

[50] P. C. Hariharan, J. A. Pople, *J. Theor. Chim. Acta* **1973**, *28*, 213.

[51] A. E. Reed, L. A. Curtiss, F. Weinhold, *Chem. Rev.* **1988**, *88*, 899.

[52] a) E. Runge, E. K. U. Gross, *Phys. Rev. Lett.* **1984**, *52*, 997; b) M. Petersilka, U. J. Gossmann, E. K. U. Gross, *Phys. Rev. Lett.* **1996**, *76*, 1212; c) M. E. Casida, M. Huix-Rotlant, *Annu. Rev. Phys. Chem.* **2012**, *63*, 287.

[53] A. Vlček, S. Zalis, *Coord. Chem. Rev.* **2007**, *251*, 258.

[54] J. Tomasi, B. Mennucci, R. Cammi, *Chem. Rev.* **2005**, *105*, 2999.

Received: March 2, 2016
Published Online: May 19, 2016